

Application for Analysis of the Multiple Coherence Function in Diagnostic Signal Separation Processes

Mariusz WĄDOŁOWSKI

*Warsaw University of Technology, Faculty of Automotive and Construction Machinery
Engineering, Institute of Machine Design Fundamentals, L. Narbutta 84,
02-524 Warsaw, mariusz.wadolowski@pw.edu.pl*

Jarosław PANKIEWICZ

*Warsaw University of Technology, Faculty of Automotive and Construction Machinery
Engineering, Institute of Machine Design Fundamentals, L. Narbutta 84,
02-524 Warsaw, jaroslaw.pankiewicz@pw.edu.pl*

Damian MARKUSZWESKI

*Warsaw University of Technology, Faculty of Automotive and Construction Machinery
Engineering, Institute of Machine Design Fundamentals, L. Narbutta 84,
02-524 Warsaw, damian.markuszewski@pw.edu.pl*

Abstract

Diagnosing the condition of the machine during its operation by non-invasive methods is most often reduced to measuring the acceleration of vibrations occurring on the housing, as close as possible to the observed element or changes in sound pressure in the immediate vicinity of the machine. For proper inference about the condition of a given machine element, the registered signals should be undisturbed by signals coming from other components and free from external interference. In the case of simple stationary machines, it is quite simple, but in the case of more complex systems, such as a car, which in addition is in motion, things get complicated. In the available literature we find examples of the effectiveness of using ordinary coherence function to separate signals from two independent sources [1,2,3]. This work presents attempt to build an algorithm that uses signals from a multi-point measurement system to analyze multiple coherence functions, which allows to separate signals from various sources. It can then get diagnostic information from the signal thus separated. The effectiveness of the algorithm was tested on a model simulating signal mixing, and then using signal coherence function and knowledge of the transmittance function, the signals were separated.

Keywords: partial coherence, signal separation, machine diagnostics

1. Introduction

The progress of digital technology has enabled an increase in the computing power of computers and thus it has become possible to use simulation methods to create, calculate and process signals based on complex mathematical models. The mathematical model of the system is a reflection of physical phenomena in mathematical relations between the input and output of the model. Built simple models with increasing accuracy reflect phenomena occurring in real physical objects, which are confirmed by experimental verifications.

In real complex systems, e.g. a car, this consists of many elements such as: engine, gearbox, suspension system, etc. The vibroacoustic signal is generated by various elements of the system, e.g. gear wheel cooperation, crankshaft rotation, ignition, etc. These elements we can consider as source. Unfortunately, direct measurement of source signals is impossible. From here, we try to measure the source as close as possible. For multi-source systems, measurements should be made at least as many observation points as there are sources. If we assume independent linear propagation paths between the source and the output point Figure 1,[4] and assume that the signal from the observation point is equal to the source signal [5], then the ordinary coherence function between the source signal and the output signal $y(t)$, will estimate as a part of the signal $x_n(t)$ is in the signal $y(t)$ for a given frequency f .

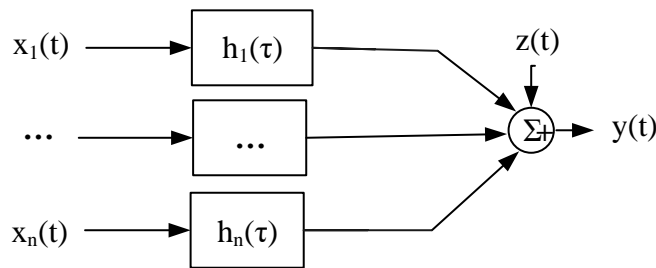


Figure 1. Multi-line / single-output linear system

Equation (1) describes the ordinary coherence function.

$$\gamma_{xy}^2 = \frac{H^{(1)}}{H^{(2)}} = \frac{|S_{xy}|^2}{S_{xx} \cdot S_{yy}}, \tag{1}$$

where: S_{xy} - cross spectral density of the signal $x(t)$ and $y(t)$, S_{xx}, S_{yy} - two-sided spectral density of the signal $x(t), y(t)$, $H^{(1)}, H^{(2)}$ - transmittance of the system $H^{(1)} = \frac{S_{xy}}{S_{xx}}, H^{(2)} = \frac{S_{yy}}{S_{yx}}$

In most cases, complex systems are not as simple as shown. Source signals $x_n(t)$ are recorded in all output signals in various proportions described by equation (3). The proportions depend on the function of the transition between the source and the observation point. As the distance increases, the source part in the $x_n(t)$ signal decreases Figure 2.

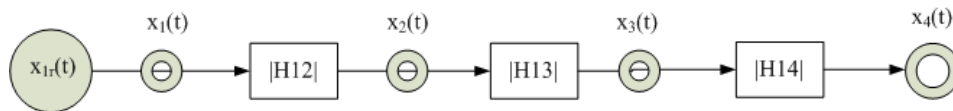


Figure 2. Signal propagation path $x_n(t)$ and observation points

The ordinary coherence function calculated from such signals causes erroneous inference, as to the origin and value of source signals [6] and therefore, such a signal is not suitable for diagnostic use. It is necessary to use a signal separation algorithm, that will enable the source signals to be reproduced based on the knowledge of the output signals.

Several separation techniques exist. The main difference is in the field of activity [7]. Signal separation can be done in the time or frequency domain. The article discusses the separation of signals in the frequency domain using the partial coherence method.

2. Construction of the signal mixing model

The built model of the system can consist of any number of input signals $x_{nr}(t)$, described by any functions Figure 3. In the assumed algorithm, to more accurately reflect real systems, the signal was described by a polyharmonic function modulated by another harmonic function (2).

$$x_{nr}(t) = A(t) \cdot \cos(2\pi \cdot f_n + \phi(t)) \tag{2}$$

where: $A(t)$ - amplitude modulation function, $\phi(t)$ - phase modulating function
 f_n - frequency characterizing the signal

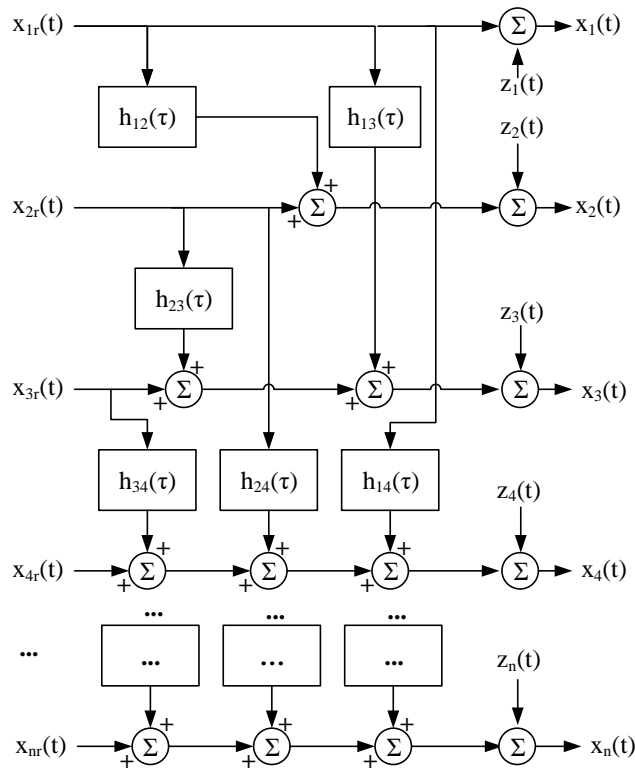


Figure 3. Model diagram of signal mixing

The number of output signals $x_n(t)$ should be the same as the input. In addition, between the input and the output of the same signal pairs, the transition function $h_{nn}(\tau)=1$.

Additionally, noise $z_n(t)$ was added to the output signals. The output signals are the sum of the respective input signals and their transition functions $h_{ni}(\tau)$:

$$x_4(t) = x_{4r}(t) * h_{44}(\tau) + x_{1r}(t) * h_{14}(\tau) + x_{2r}(t) * h_{24}(\tau) + x_{3r}(t) * h_{34}(\tau) + z_4(t) \quad (3)$$

Sample graphs of gain factors are shown in Figure 5.

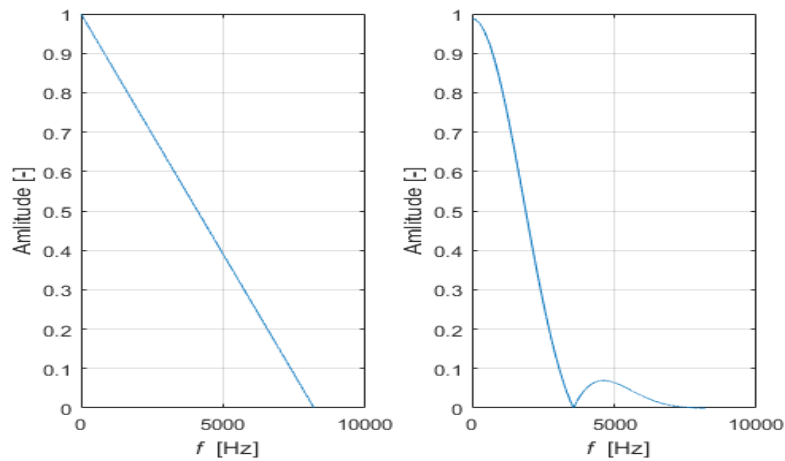


Figure 4. Gain factor (transmittance) $|H_n(f)|$

In the further part of the model considerations, an example was considered for four input signals and four output signals (observation points). Polyharmonic signals $x_{nr}(t)$ were generated and linear transformations were made for various transmittances $h_{ni}(\tau)$. As a result of these calculations, the output signals $x_n(t)$ were obtained. Only knowledge of these signals were assumed for further calculations. The spectrum of the signals $x_{nr}(t)$ and the mixed signal $x_4(t)$ are shown in Figure 5.

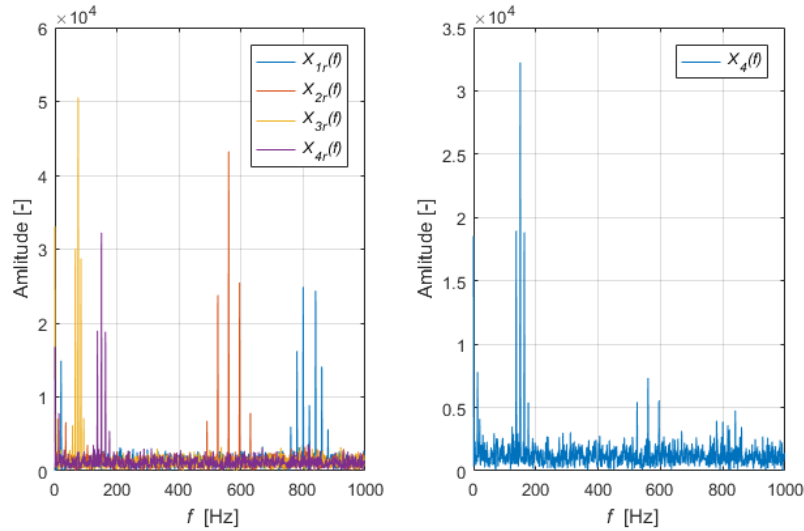


Figure 5. Spectral density of input (source) signals and output signal $x_4(t)$

3. Signal separation

For linear systems, the ordinary coherence function γ_{xy}^2 can take values $\langle 0 \text{ to } 1 \rangle$, where 1 means that the signals are coherent and 0 means no coherence. For such adopted values we can assume that each non-coherent part of the signal comes from external interference (noise) or from other sources in the system. When calculating the ordinary coherence function between the output signals $x_1(t)$, $x_2(t)$, $x_3(t)$, $x_4(t)$ we note that the value of the function is falsely inflated by signals from other sources. To eliminate the overstated value, the partial coherence function was calculated, which consists in eliminating from both signals a part from other sources (4,5,6,7) [8]. The logical diagram of the calculations for four inputs and four outputs is shown in Figure 6.

$$\gamma_{y:1}^2 = 1 - [1 - \gamma_{1y}^2] = \gamma_{1y}^2 \tag{4}$$

$$\gamma_{y:2!}^2 = 1 - [(1 - \gamma_{1y}^2) \cdot (1 - \gamma_{2y \bullet 1}^2)] \tag{5}$$

$$\gamma_{y:3!}^2 = 1 - [(1 - \gamma_{1y}^2) \cdot (1 - \gamma_{2y \bullet 1}^2) \cdot (1 - \gamma_{3y \bullet 2!}^2)] \tag{6}$$

$$\gamma_{y:q!}^2 = 1 - \prod_{i=1}^q (1 - \gamma_{iy \bullet (i-1)!}^2) \tag{7}$$

Where: y – signal sought, $q!$ - number of subtracted signals

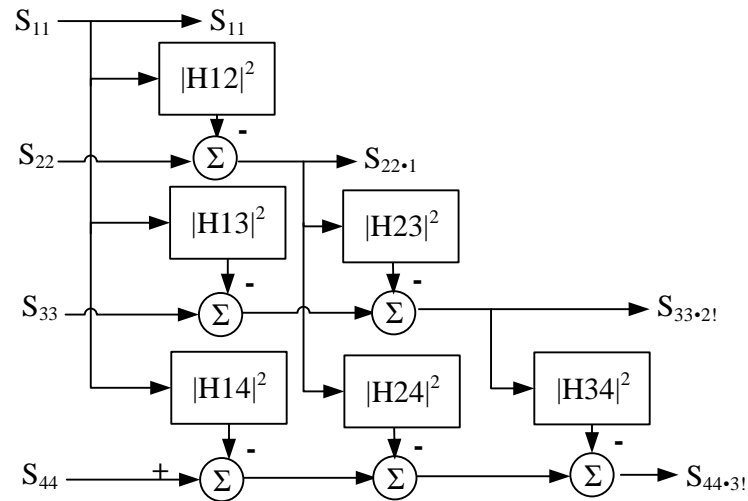


Figure 6. Signal separation diagram

The residual spectral density of the variable y was calculated from the relationships:

$$S_{yy \cdot 1} = [1 - \gamma_{1y}^2] \cdot S_{yy} \tag{8}$$

$$S_{yy \cdot 2!} = [1 - \gamma_{y:2!}^2] \cdot S_{yy} \tag{9}$$

$$S_{yy \cdot q!} = [1 - \gamma_{y:q!}^2] \cdot S_{yy} \tag{10}$$

For the calculations polyharmonic input signals $x_n(t)$ were assumed, consisting of two different frequencies in which one is modulated by the other. The frequencies are in the range of 0-1000 Hz. The source signal sample length consists of $2^{14} \cdot 60$ points. 2^{14} points were used for the analysis, from which the Fourier transform was calculated and averaged with the 60% overlap. Then, between the output signals, the partial coherence (7) was calculated and the spectra of the input signals (10) were reproduced. They were compared with the assumed source signals and the results obtained are presented in Figures 7.

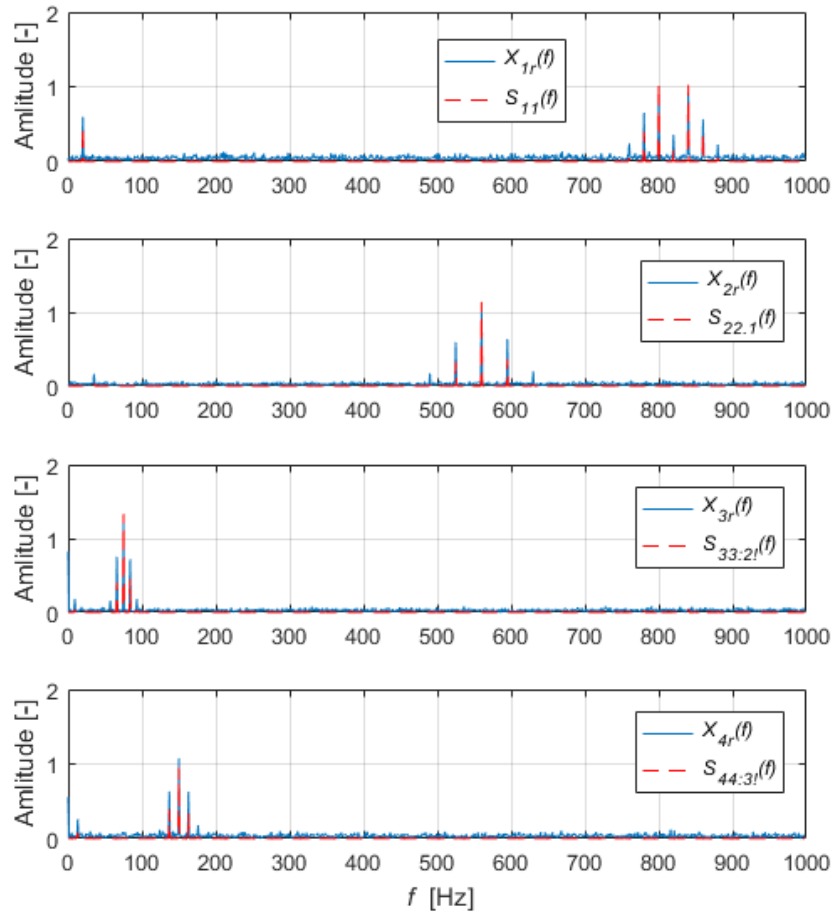


Figure 7. Spectral density of source signals and separated signals

4. Conclusions

After starting the digital algorithm, the signals were automatically separated and compared with the input signals. It was found that with such assumptions, the approximation error is so small that even such a simple algorithm works correctly. Based on the knowledge of only output signals, we are able to separate a signal that can be used as a diagnostic symptom.[9,10,11] Figure 7 will show the input signals and their corresponding separated signals.

References

1. J. Dziurdź, *Application of correlation and coherence functions in diagnostic systems*, Solid State Phenomena, 196 (2013) 3-12.
2. Z. Dabrowski, J. Dziurdz, D. Górnicka, *Utilisation of the Coherence Analysis in Acoustic Diagnostics of Internal Combustion Engines*, Archives of Acoustics, 42 (2017) 475-481.
3. J. Dziurdź, *Separacja składowych widmowych w zadaniu identyfikacji modelu nieliniowego*, Diagnostyka, 30 (2004) 162-166.
4. M. R. Reksoprodjo, W. Nirbito, *Characteristics of Vibration Propagation on Passenger Car Monocoque Body Structure at Static Small Turbocharged Diesel Engine Speed Variation*, Journal of Physics: Conference Series., 1519 (2020) 012005.
5. Z. Zhang, D. Pan W. Wu, C. Huang, *Vibration source identification of a heavy commercial vehicle cab based on operational transfer path analysis*, Proceedings of the Institution of Mechanical Engineers, Part D: Journal of Automobile Engineering, 234 (2020) 669-680.
6. Y. Pan, Y. Li, M. Huang, Y. Liao, D. Liang, *Noise source identification and transmission path optimisation for noise reduction of an axial piston pump*, Applied Acoustics, 130 (2018) 283-292.
7. R. Szupiluk, P. Rubach, *Metodyka i praktyka filtracji opartej na ślepej separacji sygnałów*, Roczniki Kolegium Analiz Ekonomicznych/Szkoła Główna Handlowa, 2019, 183-195.
8. J.S. Bendat, A. G. Piersol, *Random data: analysis and measurement procedures*, John Wiley & Sons, 2011.
9. F. Berlato, G. D'elia, M. Battarra, G. Dalpiaz, *Condition monitoring indicators for pitting detection in planetary gear units*, Diagnostyka 21 (2020).
10. A. Taghizadeh-Alisarai, A. Mahdavian, *Fault detection of injectors in diesel engines using vibration time-frequency analysis*, Applied Acoustics, 143 (2019) 48-58.
11. B.J. Krężel, P. Białkowski, *Diagnostic of shock absorbers during road test with the use of vibration fft and cross-spectrum analysis*, Diagnostyka, 18 (2017) 79-86.